

# pQCT-assessed relationships between diaphyseal design and cortical bone mass and density in the tibiae of healthy sedentary and trained men and women

R.F. Capozza<sup>1</sup>, J. Rittweger<sup>2</sup>, P.S. Reina<sup>1</sup>, P. Mortarino<sup>1</sup>, L.M. Nocciolino<sup>1</sup>, S. Feldman<sup>3</sup>, J.L. Ferretti<sup>1</sup>, G.R. Cointry<sup>1</sup>

<sup>1</sup>Center of P-Ca Metabolism Studies (CEMFoC), and <sup>3</sup>LABOATEM, Faculty of Medicine, National University of Rosario, Argentina;

<sup>2</sup>German Space Agency (DLR), Cologne, Germany

## Abstract

In a pQCT study of running-trained and untrained men and women we had shown that bone mass distribution along the tibia was adapted to the usage-derived stress pattern. To study the possible association between the efficiency of diaphyseal design and bone material stiffness, we extend the analysis of the same sample to correlate pQCT indicators of the distribution (CSMIs), mass (BMC), and density (vBMD) of cortical bone tissue as descriptors of “distribution/mass” (d/m) or “distribution/quality” (d/q) relationships. The d/m and d/c curves followed positive (exponential) and negative (hyperbolic-like) equations, respectively. Distribution curves of r coefficients throughout the bone were all bell-shaped, reaching a maximum towards the mid-diaphysis. The CSMIs and BMC were higher, and vBMD was lower in men than women and in runners than non-runners. The d/m relationships were described by unique curves for all groups while d/q relationships were better adjusted to separate curves for men and women. Results support that: 1. diaphyseal design reflects the relative influence of bending/torsion stress along the bones, tending to minimize bone mass; 2. there is a trade-off between cortical bone “quality” and distribution; 3. d/m and d/q relationships are related to bone mechanical environment, and 4. d/q relationships are affected by sex.

**Keywords:** Bone Biomechanics, pQCT, Osteoporosis, Bone Density, Bone Structure

## Introduction

In tubular bones, the structural stiffness is determined exclusively by the specific stiffness (elastic modulus) and the spatial distribution of bone tissue<sup>1-4</sup> (Figure 1a). Bone tissue stiffness, chiefly determined by genetic factors, depends on tissue mineralization and tends to vary relatively little (generally within the same order of magnitude) between different regions of the same bone<sup>5-18</sup>. However, the mechanical<sup>14</sup> and metabolic environments of bones<sup>18</sup> can also affect bone tissue

micro-porosity (cell lacunae, vascular channels, Haversian remodeling, microdamage). Cortical tissue distribution can vary widely as a function of the stress determined by load-bearing. In long bones stressed in uniaxial *compression*, diaphyseal strength depends chiefly on the bone *mass* present in the perpendicular bone cross-section. When *bending or torsional* moments contribute to bone load, diaphyseal strength will increase with the *distance* of cortical tissue from the neutral axis, as technically described by the axial and polar *cross-sectional moments of inertia (CSMIs)*, respectively<sup>2-4</sup>.

The CSMIs can only be modified by a directional orientation of periosteal bone formation and/or endocortical resorption (Frost’s *modeling drifts*). Bone mechanostat is a feedback mechanism that regulates bone structural stiffness by orienting modeling drifts as determined by the usage-induced bone strains<sup>5,6,19-22</sup>. The system tends to homogenize bone strain distribution in dynamically equivalent bone sites (Figure 1b), suggesting that *the way the tissue is distributed within a bone is quite as important as the volume of material*<sup>6,23</sup>. This would involve a trade-off between stiffness and mass, or between ma-

The authors have no conflict of interest.

Corresponding author: Dr. Gustavo Cointry, Colón 1929 Depto 2, Rosario, 2000, Argentina

E-mail: gcointry@gmail.com

Edited by: F. Rauch

Accepted 18 April 2013

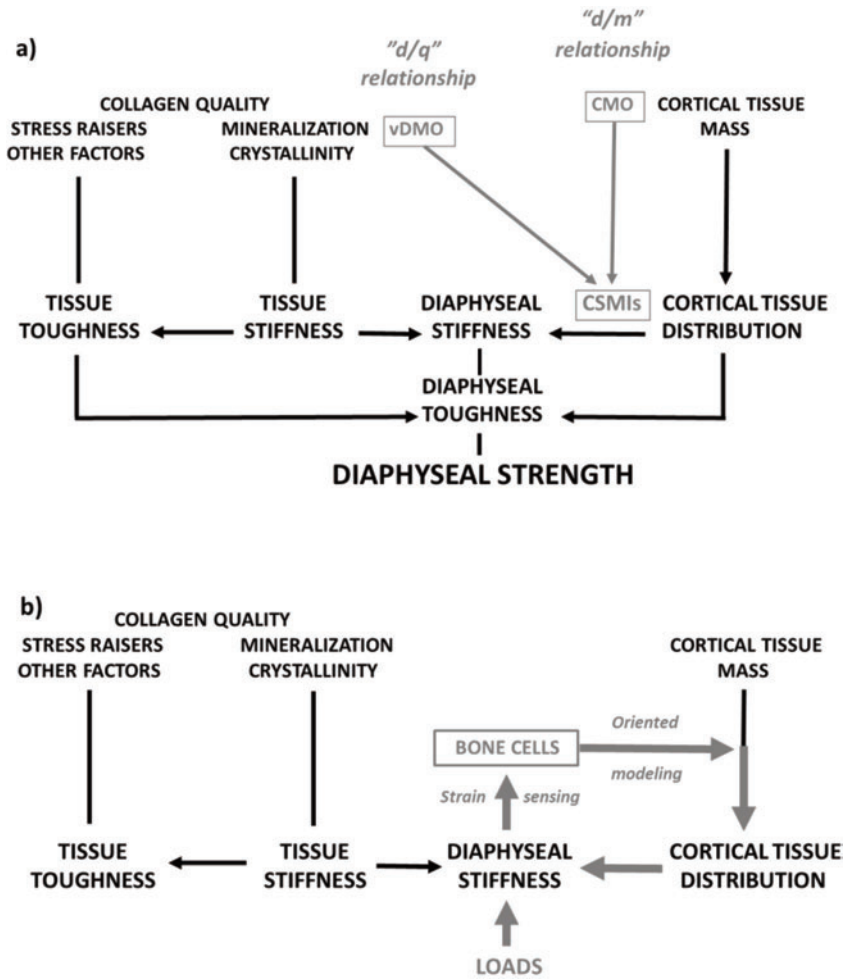


**Figure 1. a.** Schematic representation of the biological determination of the mechanical quality of cortical bone tissue (left column) and the spatial distribution of that tissue (right column) to conform the structural stiffness, toughness and strength of long-bone diaphyses as combined outputs. In a central column (in grey), the pQCT indicators of cortical bone tissue mass (BMC), distribution (CSMI's) and "quality" (volumetric BMD) determined in this study as descriptors of the relationships involved in the d/m and d/q associations are also indicated. **b.** Representation of the proposed feed-back system (bone *mechanostat*) that would control structural bone stiffness as a function of the strains provoked by the loads usually supported by the bone, within an analogous scheme to that sketched in (a).

terial and geometric properties<sup>1,4,5</sup> which would tend to *maximize the CSMI/mass relationship* in bones loaded in bending or torsion<sup>1</sup>. Thus, the efficiency of bone *mechanostat* could be described by how well every available unit of cortical bone mass is utilized to optimize the cross-sectional design as a function of the supported compression (mass), or bending of torsion loads (CSMIs)<sup>4,24</sup>, with some expected site specificity<sup>20,25-27</sup>. In this study, such associations are regarded as "*distribution/mass*" (d/m) relationships (Figure 1a). The modeling response to mechanical stimuli should also grow *as a function of bone tissue deformability* at every site<sup>26,28,29</sup>. That kind of association could be described by *inverse relationships* between the bending or torsion CSMI's and the specific stiffness of bone tissue in different bone sites. In this study, such associations are regarded as "*distribution/quality*" (d/q) relationships (Figure 1a).

The pQCT technology can determine indicators of cortical bone mass, volumetric density, and distribution<sup>30</sup> (Figure 1a), and hence analyze the abovementioned relationships (Figure 1b). However, that kind of investigation has largely been overlooked<sup>18</sup>. We have demonstrated an inverse relationship between tomographic and mechanical indicators of bone material and geometric properties in different instances<sup>31-40</sup>. In the present study, we aim to describe and interpret some d/m and d/q relationships at the tissue and organ levels of complexity by extending the analysis of the pQCT indicators of tibial cortical bone mass, volumetric density and distribution previously obtained in healthy sedentary individuals and in trained runners<sup>38,40</sup>. With that purpose, we studied the relationship between bending and torsion CSMI's (Y) with indicators of the cortical mass (BMC, X<sub>1</sub>), to analyze the corresponding d/m curves, and with indicators of the mineralization of cortical tissue (as assessed by its volumetric

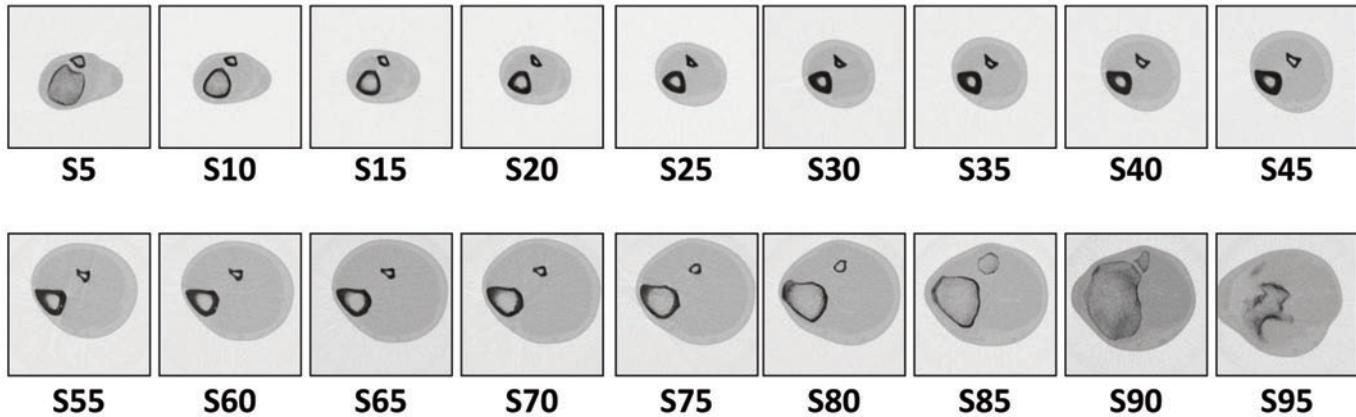


**Figure 2.** Serial scans obtained at regular intervals equivalent to 5% of the tibia length from the joint line of the heel, as described in the text. Scans are numbered from “S5” (taken at a 5% distance from the heel) to “S95” (taken at a 95% distance from the heel).

BMD ( $X_2$ ), a linear correlate of its intrinsic stiffness<sup>3</sup>), to analyze the corresponding d/q curves. We hypothesized that: 1. in those conditions, the observed d/m relationships should be described by positive relationships, and the d/q relationships by negative relationships, and 2. the adjustment of the data to the corresponding correlation curves should be more significant toward the center regions of the bones than toward the bone ends, as an expression of the bone design adaptation to bending or torsion stresses which are known to be progressively predominant toward the mid-diaphysis<sup>22,38,40</sup>. In addition, the study aimed to describe the effect of the degree of physical activity of the individuals, and the eventual interference of sex-related factors on the d/m and d/q relationships in the assayed conditions.

## Material and methods

**The study participants.** The study included 10 men and 12 women, all healthy and with sedentary habits (untrained individuals), and 10 male and 14 female endurance runners, matched for age (sedentary/runners, men=31.9±3.1 / 33.9±3.2 yr; women=30.9±3.2 / 31.3±3.9 yr; ANOVA: n.s.), weight (men=79.7±10.7 / 78.6±4.4 kg; women=56.1±2.5 / 54.5±4.3 kg; ANOVA: n.s.) and height (men=176.1±3.2 / 174.7±2.9 cm; women=164.0±1.8 / 160.5±5.0 cm; ANOVA: n.s.). All runners had engaged in regular long-distance running comprising 3-5 sessions per week, 10-15 km per session, for 8 years or longer, at an average velocity of 11.9±0.5 km/h for men and 10.6±0.7 km/h for women. None of the participants had a history of fractures or diseases, smoking or drinking, or treatments affecting the skeleton, and none of the women had a history of menstrual disorders. Informed consent was obtained by each individual before inclusion in the study. The study has been approved by the Hospital’s Ethics Committee [Application # 83, *Comité de Ética, Hospital Provincial del Centenario*, Rosario, Argentina].

**pOCT Measurements.** The entire right tibia of each individual was scanned with an XCT-2000 scanner (Stratec, Germany). The

radiation dose involved a total body equivalent dose of 0.9  $\mu$ Sv per scan, with a cumulative dose for the whole study in the order of 20  $\mu$ Sv. The X-ray beam generated by the XCT-2000 scanner had a thickness of 2.5 mm, and the pixel edge size was set to 0.5 mm. Cross-sectional images were obtained at regular intervals equivalent to 5% of the tibia’s length. Scans were numbered from S5 (5% site, next to the tibia-talar joint) to S95 (95% site, next to the knee joint). For technical reasons, the scan at S50 could not be obtained in any case. Thus, a total of 18 scans were obtained for the entire bone (Figure 2). All image analyses were done with the integrated XCT software in its version 5.50. The following parameters were applied for all sectional images: *contmode 2*, *peelmode 2*, and *cortmode 1*. Threshold values for total and cortical bone were selected at 398.5 and 700.0  $\text{mg}\cdot\text{cm}^{-3}$ , respectively. The following indicators were obtained from each scan<sup>30,41</sup>.

**Bone “mass” indicator:** *Mineral content of cortical bone (Cortical BMC):* amount of mineral present in the defined cortical bone area of the tibia cross-section, in mg per mm of slice thickness.

**Diaphyseal design indicators:** *Second moments of inertia of the cortical area (cross-sectional moments of inertia, CSMI’s):* integrated sums of products of the area of every pixel in the defined cortical image by its squared perpendicular distance to one of three selected, neutral bone axes passing through the center of mass of the bone image, namely: the longitudinal axis (polar or torsion CSMI, pCSMI); the lateral-medial axis (anterior-posterior (A-P) bending CSMI, xCSMI); and the anterior-posterior axis (lateral bending CSMI, yCSMI), in  $\text{mm}^4$ . These measures capture the architectural efficiency of the cross-sectional design of the cortical shell to resist torsion and bending in the frontal and sagittal planes, respectively<sup>24</sup>. The xCSMI and yCSMI values were calculated after rotating the axis system on the image until achieving a maximal (y) value, as the perpendicular axis to (x) passing through the center of gravity.

**Bone material “quality” indicator:** *Volumetric mineral density of cortical bone (cortical vBMD)=cortical BMC / cortical area*, in  $\text{mg}\cdot\text{mm}^{-3}$ : It expresses the amount of mineral per

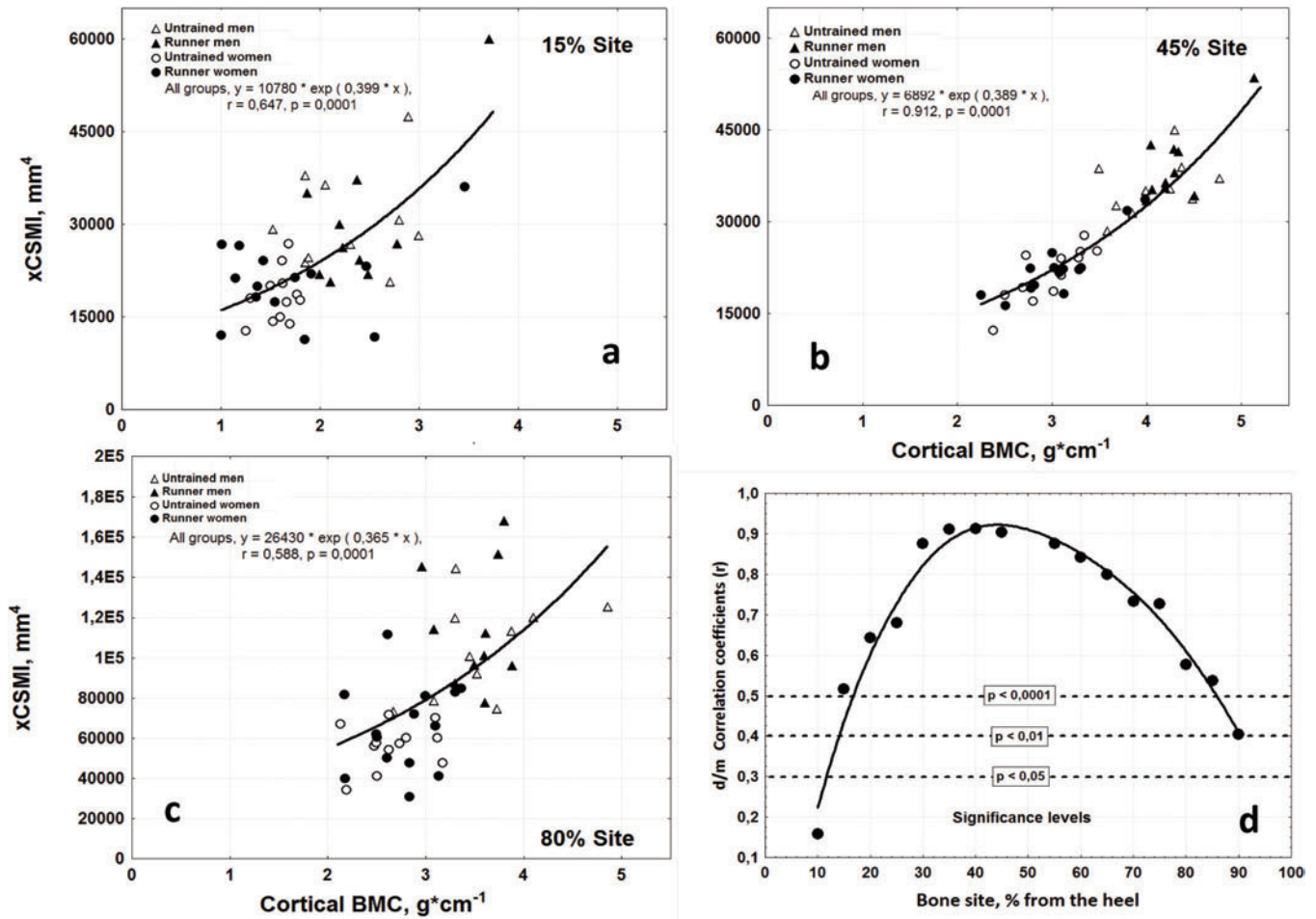


**Figure 3.** “Distribution/mass” (d/m) relationships observed between the xCSMI and cortical BMC values of all the individuals studied together, determined at some representative sites of the tibiae: **a.** at S15; **b.** at S45; **c.** at S80, as indicated and explained in the text. The best-fit, exponential equations and the statistical adjustment of the corresponding correlations are indicated. Graph **(d)** shows the distribution of the correlation coefficients (r) values of all the “distribution/mass” (d/m) relationships, analyzed as shown in **a,b,c** (ordinates), calculated for each of the studied sites (abscissae). The  $p < 0.05$ ,  $p < 0.01$  and  $p < 0.001$  levels of statistical significance of the respective correlations are indicated.

unit of cortical bone volume including the pores (apparent volumetric density), a variable which is known to vary in direct proportion with the intrinsic stiffness (elastic modulus) of cortical bone tissue<sup>5</sup>. In order to minimize the measurement error derived from the “partial volume effect” unavoidably produced by pixels not fulfilled with bone tissue<sup>42</sup>, the cortical vBMD was determined only in those images showing a cortical thickness larger than 3 times the pixel edge length (in practical terms, in every image from S10 to S90, the cortical thickness being always larger than 5 pixels from S20 to S80).

**Statistical analyses.** Simple correlation analyses [*Statistica software; Statsoft, USA*] were performed between the xCSMI, yCSMI or pCSMI values (ordinates) and the cortical BMC or vBMD data (abscissae) of all the individuals studied together per each scan obtained, from S10 to S90. The curves obtained this way were regarded as describing “distribution/mass” (d/m, CSMI’s vs cortical BMC) and “distribution/quality” (d/q,

CSMI’s vs cortical vBMD) relationships, respectively. The best-fit equations to describe the behavior of the d/m and d/c curves were obtained with the aid of *Mathlab software [Math-Works, USA]*. The calculated correlation coefficients (r) of all the d/m and d/q correlation curves obtained were plotted per bone site to describe the particular distributions of their values throughout the bone. Taking profit of the similitude of the slopes of the d/q relationships obtained at each site studied in the central region of the bones, they were additionally evaluated for the data from all the groups together in all sites within the two central quarters of the bone length (i.e. from S25 to S75). A similar analysis was applied to the sites of the distal and proximal quarters where the d/q correlations were found statistically significant (as indicated in each case), for comparative purposes. ANCOVA tests were employed to evaluate the differences between heights and slopes of the curves for men and women data, as needed.

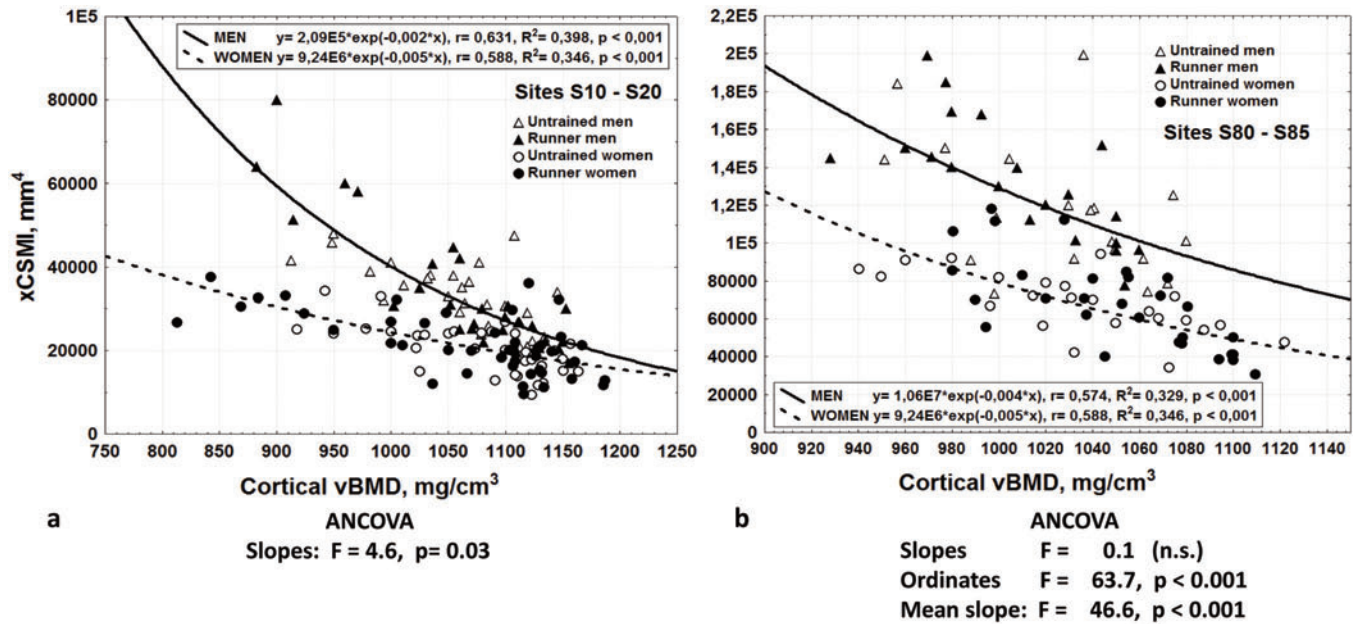


**Figure 4.** “Distribution/quality” (d/q) relationships observed between the xCSMI and cortical vBMD values of the men (triangles) and women (circles) groups, determined for sites S10 to S20 (a) and for sites S80 and S85 (b) of the tibiae as indicated and explained in the text. Sedentarian (open symbols) and runner (full symbols) individuals were grouped within sex. The best-fit, negative exponential equations describing the adjusting curves for each sex and the statistical significance of the respective correlations and the ANCOVA-tested difference in height between the curves are indicated.

## Results

### *CSMI's, cortical BMC and cortical vBMD values analyzed per bone site*

All the CSMI's grew exponentially in the proximal sense from S35 upwards. They were all significantly higher in men than in women, as well as in runners than in sedentarians (always  $p < 0.001$ ). In particular, the xCSMI's were significantly greater in runner than in sedentary individuals from S35 upwards, with larger differences shown within men ( $F = 21.0, p < 0.0001$ ) than within women ( $F = 8.0, p < 0.005$ ). Cortical BMC increased more than twofold from S10 to S45 in all groups and fell proximally by about the same amount from S55 to S90. It was also always higher in men than in women, as well as higher in runner than in sedentary men from S10 to S45 ( $F = 45.2, p < 0.0001$ ), with little or no difference within the women. A similar behavior was observed for the cortical thickness. Cortical vBMD was higher in the distal than in the proximal half of the bones in all groups ( $p < 0.01$ ) and was always higher in women than in men ( $p < 0.001$ ). It was also always lower in runners than in sedentarians in both sexes, with significant differences between S60 and S75 (men,  $F = 14.6, p = 0.0003$ ; women,  $F = 15.5, p < 0.0002$ ).

### *“Distribution/mass” curves*

Significant correlations were observed between either of the CSMI's and the cortical BMC of all the individuals studied at each

scanned site, all of them described by positive, exponential functions. Prototypical examples of these relationships for the xCSMI taken at sites S15, S45 and S80 are given in Figure 3. In all the graphs, the data from men tended to be located toward the higher-right region of the graphs, while those from the women were toward the lower-left region. Despite of this fact, the whole d/m relationships could always be described by unique curves for all the individuals together, regardless of sex and degree of physical activity, and as such they were analyzed thereon.

A regional analysis of the d/m curves along the bones showed some significant site specificity:

1. Toward the distal end of the tibia (S5-S15), the d/m relationships were little or no significant and showed quite low slope values. A prototypical relationship for the xCSMI at S15 (at which the significance of the association was maximal for the selected region) is shown in Figure 3a. From S20 to S35 the statistical significance and the slopes of the d/m relationships increased progressively, yet still showing relatively low slope values.
2. Between S30 and S60-65, highly significant correlations of the d/m curves were observed, with correlation coefficients always over 0.80 (determination coefficients  $R^2$  always over 0.64) and progressively higher slopes. A prototypical curve for the xCSMI at S45 is shown in Figure 3b.
3. Going proximally from S65, the d/m relationships rapidly loose statistical significance, yet showing always the typical positive, exponential behavior. A prototypical curve for the xCSMI at S80 is shown in Figure 3c.

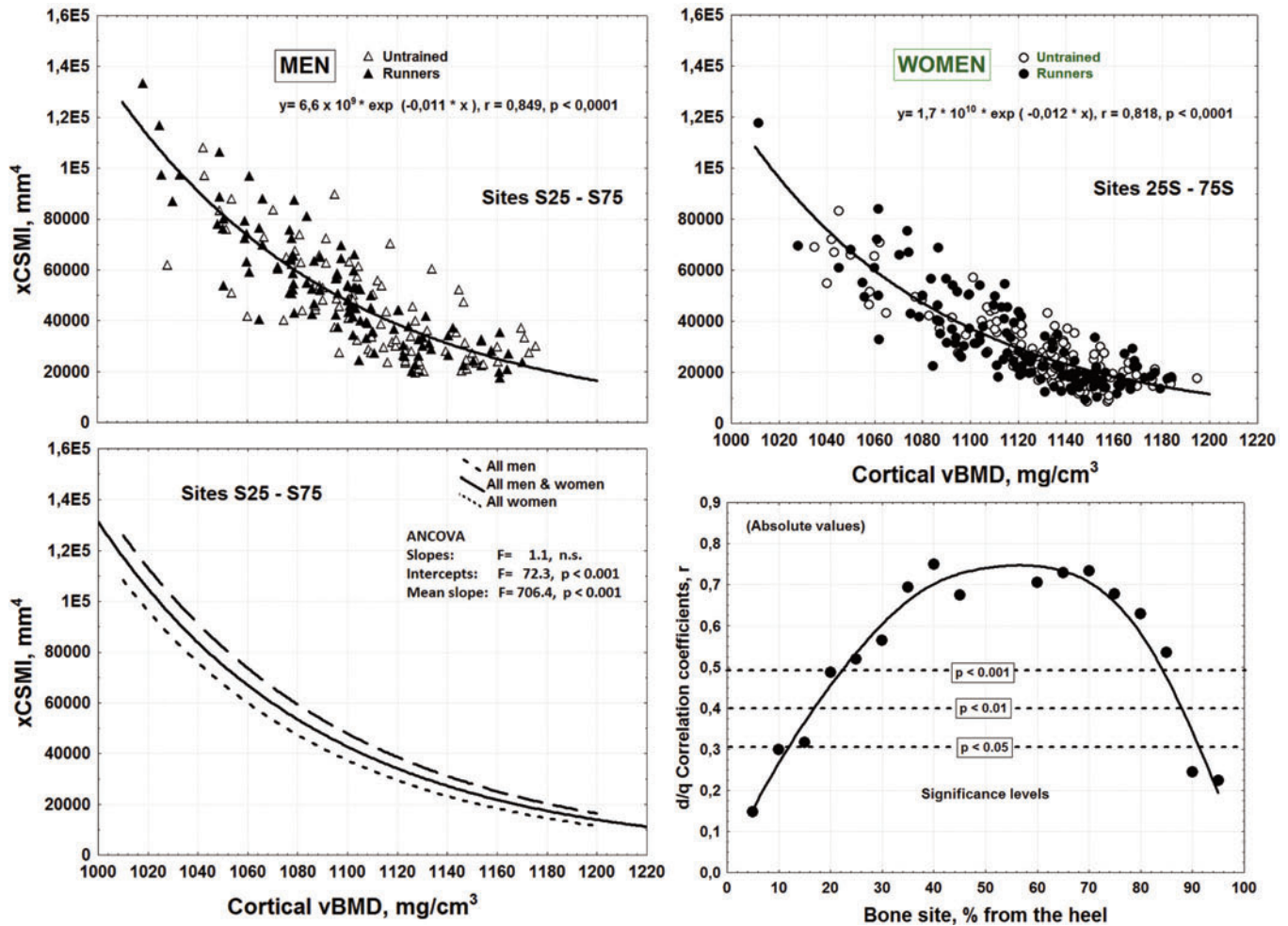


**Figure 5.** “Distribution/quality” (d/q) relationships observed between the xCSMI and cortical vBMD values of the men (a) and women (b) groups, determined from sites S25 to S75 of the tibiae as indicated and explained in the text. Sedentarians (open symbols) and runners (full symbols) were grouped within sex. The best-fit, negative exponential equations describing the d/q curves and the statistical significance of the respective correlations are indicated. Graph (c) shows the isolated curves describing the d/q relationships for men and women as shown in graphs (a) and (b), the ANCOVA-assessed statistical significance of the difference in height between the curves, and the single curve describing the association between the same indicators at the same sites calculated for all the individuals together. Graph (d) shows the distribution of the correlation coefficients (r) values of the “distribution/quality” (d/q) relationships analyzed for all the individuals together as shown in (c), calculated for every studied site from S10 to S90. The p<0.05, p<0.01 and p<0.001 levels of statistical significance of the respective correlations are indicated.

The distribution of the values of the correlation coefficients (r) of the d/m curves obtained throughout the bones, plotted site-by-site for each of the CSMI’s, revealed similar trends to achieve maximal values toward the mid-diaphyseal regions (roughly between S30 and S60). The corresponding distribution curves of the regression coefficient values of the d/m curves along the whole tibiae showed always a bell shape with quasi-symmetrical decays toward the distal and proximal ends of the bones, for every CSMI studied. As an example of this prototypical behavior, Figure 3d shows the distribution curve of r values calculated for the d/m relationships observed for the xCSMI of all the individuals studied together at every site scanned.

“Distribution/quality” curves

The relationships observed between either of the CSMI’s and the cortical vBMD of all the individuals studied at each scanned site were all described by negative, simil-hyperbolic correlation curves, which were best adjusted by negative exponential functions of the form  $y = a * \exp(-b * x)$  in every case. In general terms, men’s curves tended to be above those of the women. As observed with the d/m curves, there were also specific distribution zones for the data from different groups. The CSMI’s values tended to be higher, and the cortical vBMD values to be lower, in men than women, as well as in runner than sedentarian individuals within each sex.

In addition to this general behavior of the data, some important regional differences were observed in the d/q relationships along the bones.

1. Toward the distal end of the tibia (S10-S20), the d/q relationships for any of the studied CSMI's showed a relatively large dispersion of the data. However, the similarity of the slopes of the curves within each sex allowed grouping the data taken at different sites, which were described by separate, significant single curves for men and women, though with different slopes for each sex (Figure 4a).
2. Between S25 and S75 the statistical significance of the d/q relationships increased progressively up to achieve quite high correlation coefficients. Again, the similarity of the slopes within sex allowed analyzing the whole sets of data obtained in all the included sites for each sex by separate. High correlation and determination coefficients were obtained in every case (Figures 5a,b). In this region, as expected, the cortical vBMD values for men plotted significantly lower than those shown by the women, and the CSMI's plotted significantly higher for the men. Nevertheless, the separate adjusting curves for men's and women's data were always virtually parallel and showed a significant but relatively small difference in height. Accordingly, a common adjusting curve for both sexes together was always highly significant. In the case of the xCSMI (Figure 5c), the common adjusting curve ( $r=0.927$ ,  $p<0.001$ ) plotted at a fairly constant, about 5,000 mm<sup>4</sup> difference in xCSMI value from each of the curves for men and women.
3. Going proximally, for S80 and S85 data, the d/q relationships rapidly lost statistical significance, as observed toward the distal tibia region. The graph for the xCSMI at these sites is shown in Figure 4b. The slopes of the curves for men and women remained fairly parallel, but the intercept difference tended to increase.

Accordingly, and similarly to what was observed for the d/m curves, the site-by-site distribution curves of the correlation coefficients ( $r$ ) of the d/q relationships (determined for all the individuals as a whole along the entire bones) were bell-shaped for all the CSMI's. As an example, the distribution curve of  $r$  values for the xCSMI is shown in Figure 5d.

## Discussion

**“Distribution/mass” (d/m) relationships.** Our d/m curves highlight the concept that “*for long bones, bending and torsional properties increase linearly with material stiffness and strength, and nonlinearly with increasing area*”<sup>4,6,19,23,43,44</sup>. It can be speculated: 1. that a higher/lower statistical significance of a d/m curve for a given bone section will reflect a closer/weaker association between the modeling-derived variables that define the cortical design concerning bending or torsion and the availability of cortical bone tissue in that section, and 2. that a higher/lower ordinate of a d/m curve for the same abscissa value in a particular site studied in a given individual would reflect a higher/lower ability of bone modeling to im-

prove the diaphyseal design for bending or torsion for the same amount of available cortical mass in that individual at the studied site. The fact that women followed the same d/m relationships as those shown by the men despite lower values of both BMC and CSMI's thus seems to preclude gender effects and rather suggests a common allometric function, at least for the d/m relationship. Similarly, the CSMI's and BMC values of the runners and non-runners were significantly adjusted by single d/m curves in almost all instances, likewise suggestive of a simple allometric scaling of d/m. This suggests that the high degree of physical activity of the trained men and women tended to enhance the values of both variables together following the same natural relationships, as reflecting the existence of a physiological, adaptive reaction of bone tissue to the mechanical environment in the species<sup>4</sup>, as predicted by the Mechanostat theory. This behavior is congruent with a. what was observed naturally during growth<sup>45</sup> and in the arms or legs of tennis players, triple jumpers, weightlifters, and other trained people<sup>44,46-51</sup>, and b. the need to keep the peak strains constant during either usual or enhanced physical activity, independently of bone material quality<sup>5</sup>. The bell-shaped curves in Figure 3d suggests a strikingly homogeneous trend of bone structure to concentrate the highest degree of natural biomechanical adaptation of the diaphyseal cross-sectional design to bending and torsion stresses in the tibia<sup>22,38,40</sup> as a function of the available cortical tissue toward the mid-diaphysis.

**“Distribution/quality” (d/q) relationships.** The chance for any detected bone strain at a given site to overpass the threshold for triggering bone modeling at that site should *increase* as the local tissue stiffness *decreases*, and *vice-versa*. Accordingly, the magnitude of usage-induced bone strains should be inversely related to local vBMD values at every site in the skeleton<sup>14,21,25,28</sup> (Figures 1a,b). This is what we propose as the “d/q concept”, in agreement with the hypothetical trade off between bone material quality and geometry to achieve an endpoint structural behavior<sup>3,4</sup>. In this study, the d/q relationships were always described by negative, hyperbolically-shaped functions, as usually observed when comparing any pair of variables which are mutually interrelated by a feed-back control system. We have reported similar examples of geometric compensation for decreased bone material properties<sup>8-10,12,31-36</sup>. Within the scope of the *Mechanostat* Theory, these results were among the first experimental evidences of what could be interpreted as positive (“anabolic”) or negative (“anti-anabolic”, or “catabolic”) interferences of osteoactive agents with the mechanical setpoint of the system for triggering bone modeling during growth. Other authors have also shown evidence of a similar compensation, in healthy males and females<sup>16,43,52-62</sup>, in trained individuals<sup>48,63</sup>, in *ex vivo* bone samples<sup>4,64-66</sup>, and in normal<sup>67-71</sup> and genetically-selected animals<sup>13,72-74</sup>. However, despite all that collected evidence, no attempt has been reported by other authors to describe and interpret the findings as supporting a d/q relationship or a “d/q concept” as proposed here.

Accordingly with the d/q concept, a higher correlation coefficient of a d/q curve should indicate a *closer relationship* connecting bone tissue distribution through the modeling drifts

(as assessed by the CSMI's) and bone tissue "quality" (as assessed by the cortical vBMD) in every bone site, within the general scheme of regional control of structural bone stiffness<sup>19,26,75,76</sup> (Figure 1b). It can be reasonably speculated that the ordinate value of a d/q curve for the same abscissae value of a given individual will reflect the ability of bone modeling to improve the diaphyseal design for bending or torsion for the same (local) level of tissue stiffness. In general terms, the bell-shaped curve in Figure 5d shows a similar region-specific distribution to that shown by the d/m curves (Figure 3d). In practical terms, this could be interpreted as supporting the following 3 proposals. **1.** The more deformable the bone tissue at a given point within the diaphyseal structure, the higher will be the efficiency of the modeling drifts to optimize the bone's strength as a function of the usage-derived bone strains at that site, in agreement with Currey<sup>28</sup>. **2.** That relationship should be more evident concerning bending and torsion strains and the related cross-sectional architectural adaptations toward the central region of the diaphysis than at any of the bones' ends, in agreement with Biewener & Bertram and with Ruff & Hayes<sup>22,53</sup>. **3.** The relatively small but significant gender-related differences observed in the d/q curves suggest that hormonal influences on the female skeleton could partially modify or even blunt some of the described relationships.

**General interpretation of the study.** The whole set of d/m and d/q curves obtained in this study showed a striking congruence of the observed results, especially concerning the following findings.

1. Most of the analyzed d/m and d/q relationships were highly significant. This suggests that, in general terms, the modeling-dependent distribution of the mineralized tissue within the diaphyseal cross-section at every site studied was effectively associated to both cortical bone tissue availability and deformability.
2. Single curves described the behavior of the whole sets of d/m and d/q interrelationships in all men or women studied, whatever their level of physical activity, in every instance. This suggests the existence of a common mechanism involving the interaction of bone mass and material and geometric properties within each sex (yet some gender-related differences could be detected in the d/q curves), as a function of the mechanical usage of the skeleton.
3. Both d/m and d/q curves showed virtually the same trend to achieve their maximal statistical adjustment toward the central region of the diaphysis (especially in the men). The similar distributions of the correlation coefficients of both d/m and d/q curves for all sites along the bones strongly suggest that the interaction between bone mass and material and geometric properties in long bones is maximal where bending and torsion stresses are thought to exert their maximal influence in the determination of the complex pattern of usage-derived bone strains (as long as the strength of mechanical stimulation of the bones allow for that).
4. Women tended to show all the above manifestations or relationships less evidently than men did. This particular behavior can be proposed to derive from the known effect of estrogen

to inhibit periosteal bone formation (thus minimizing the changes induced in the CSMI's) and intracortical bone remodeling (thus inducing a higher degree of mineralization - and hence of intrinsic stiffness - of cortical bone tissue).

The d/m and d/q concepts offer some interesting perspectives of clinical applications<sup>37</sup>, avoiding comparisons with samples of different, younger individuals as needed when performing DEXA studies.

**Limitations of the study. 1.** Cortical vBMD represents a combination of several bone tissue properties (degree of mineralization, porosity, osteonal density, etc.)<sup>17</sup> which are associated with the strain mode<sup>25</sup>. It is likely that each of these different properties will depict a different relationship between "density" and elastic modulus. Unfortunately, the pQCT-assessed vBMD is unable to discriminate between the independent influences of each of those factors on the degree of mineralization of the cortical tissue. Therefore, the pQCT-assessed cortical vBMD can only be regarded as a measure of bone tissue mineralization as a whole (Figure 1a). Nevertheless, this limitation does not preclude the application of a cortical vBMD value to evaluate the bone material stiffness and its contribution to the whole-bone strength as it was done in this study.

**2.** The accuracy and precision of the pQCT assessment of cortical bone properties decreases significantly when cortical thickness is lesser than 2-3 pixels of the bone image. In every analyzed image from S10 to S90 in the whole study the cortical thickness amounted more than the length of 3 pixels. However, it is unlikely that this effect would have generated the observed statistical effect, i.e. the different behavior of the d/m or d/q relationships in male (thicker) and female (thinner) bones toward the distal and proximal ends of the bones. Rather, the inherent measurement limitations will have reduced the statistical power and thus must be expected to dilute truly existing relationships.

## Conclusions

The collected evidence supports the hypothesis that, in the human leg, the modeling-dependent adaptation of the tibia cross-sectional design to the usage-induced bending or torsion strains proceeds keeping a positive (exponential) relationship with the mass of the available cortical tissue, and a negative (hyperbolic-shaped) relationship with the degree of mineralization (an indicator of the intrinsic stiffness) of that tissue.

Results suggest that the efficiency of the biological system involved in the above relationships is more evident toward the central region of the tibiae, i.e. precisely where the bending and torsion strains are thought to assume their highest influence within the complex pattern of mechanical stimulation of the bone.

In agreement with other authors<sup>49,50,77,78</sup>, it can be proposed that the existence of unique equations that significantly adjusted the different data from sedentary and trained people to single d/m or d/q correlation curves reveals that physical activity counts as a strong, natural determinant of bones' adap-



tation to the mechanical environment through changes in geometric properties, in men and women.

Within the paradigm of the Bone *Mechanostat Theory*<sup>19,26,75</sup>, the above interpretation is congruent with the idea that bones auto-control their structural stiffness through the generation of modeling drifts as a directional (i.e. vectorial) function of the mechanical usage of the skeleton (Figure 1b), with a high regional specificity.

Also within the specifications of that theory, results support the hypothesis that some non-mechanical factors (i.e. sex hormones) can influence the mechanical adaptation of the skeleton to the mechanical environment by inhibiting some modeling- or remodeling-related mechanisms involved in the biological determination of bone material and geometric properties.

Results also offer an interesting perspective for developing a non-invasive, comparative diagnosis of the functional status of bone *mechanostat* in any individual, within the limitations of pQCT technology. The curves can also assess the degree of architectural compensation of bone mass loss as a critical point at the time of defining the osteoporosis concept<sup>43,45,79</sup>.

## References

- Currey JD. What should bones be designed to do? *Calcif Tissue Int* 1984;36:S7-S10.
- McCabe F, Zhou L-J, Steele CR, Marcus R. Noninvasive assessment of ulnar bending stiffness in women. *J Bone Miner Res* 1991;6:53-9.
- Myburg KH, Zhou L-J, Steele CR, Arnaud S, Marcus R. *In vivo* assessment of forearm bone mass and ulnar bending stiffness in healthy men. *J Bone Miner Res* 1992;7:1345-50.
- Davy DT. Basic principles in bone biomechanics. *Curr Opin Orthop* 1997;8:48-57.
- Currey JD. The many adaptations of bone. *J Biomech* 2003;36:1487-95.
- Burr DB. The relationships among physical, geometrical and mechanical properties of bone, with a note on the properties of nonhuman primate bone. *Yearb Phys Anthropol* 1980;23:109-46.
- Brear K, Currey JD, Pond CM. Ontogenetic changes in the mechanical properties of the femur of the polar bear *Ursus maritimus*. *J Zool London* 1990;222:49-58.
- Ferretti JL, Spiaggi EP, Capozza RF, Cointy GR, Zanchetta JR. Interrelationships between geometric and mechanical properties of long bones from three rodent species with very different biomass: Phylogenetic implications. *J Bone Miner Res* 1992;7(Suppl.2):S423-S425.
- Ferretti JL, Capozza RF, Mondelo N, Zanchetta JR. Interrelationships between densitometric, geometric, and mechanical properties of rat femora: Inferences concerning mechanical regulation of bone modeling. *J Bone Miner Res* 1993;8:1389-96.
- Ferretti JL, Capozza RF, Mondelo N, Montuori E, Zanchetta JR. Determination of femur structural properties by geometric and material variables as a function of body weight in rats. Evidence of a sexual dimorphism. *Bone* 1993;14:265-70.
- Papadimitriou HM, Swartz SM, Kunz TH. Ontogenetic and anatomic variation in mineralization of the wing skeleton of the Mexican free-tailed bat, *Tadarida brasiliensis*. *J Zool* 1996;240:411-26.
- Di Masso RJ, Font MT, Capozza RF, Detarsio G, Sosa F, Ferretti JL. Long-bone biomechanics in mice selected for body conformation. *Bone* 1997;20:539-45.
- Jepsen KJ, Pennington DE, Lee Y-L, Warman M, Nadeau J. Bone brittleness varies with genetic background in A/J and C57BL/6J inbred mice. *J Bone Miner Res* 2001;16:1854-62.
- Van der Meulen MCH, Jepsen KJ, Mikic B. Understanding bone strength: size isn't everything. *Bone* 2001;29:101-4.
- Skedros JG, Hunt KJ, Hughes PE, Winet H. Ontogenetic and regional morphologic variations in the turkey ulna diaphysis: implications for functional adaptation of cortical bone. *Anat Rec* 2003;273A:609-29.
- Tommasini SM, Nasser P, Schaffler M, Jepsen KJ. Relationship between bone morphology and bone quality in male tibias: implications for stress fracture risk. *J Bone Miner Res* 2005;20:1372-80.
- Goldman HM, Thomas CDL, Clement JG, Bromage TG. Relationships among microstructural properties of bone at the human midshaft femur. *J Anat* 2005;206:127-39.
- Cooper DML, Ahamed Y, Macdonald HM, McKay HA. Characterising cortical density in the mid-tibia: intra-individual variation in adolescent girls and boys. *Br J Sports Med* 2008;42:690-5.
- Frost HM. The mechanostat: A proposed pathogenetic mechanism of osteoporosis and the bone mass effects of mechanical and non-mechanical agents. *Bone Miner* 1987;2:73-85.
- Cowin SC. Mechanical modeling of the stress adaptation process in bone. *Calcif Tissue Int* 1984;36:S98-S103.
- Lanyon LE, Goodship AE, Pye CJ, MacFie JH. Mechanically adaptive bone remodeling. *J Biomech* 1982;15:141-54.
- Biewener AA, Bertram JEA. Skeletal strain patterns in relation to exercise training during growth. *J Exp Biol* 1993;185:51-69.
- Cheng S, Toivanen JA, Suominen H, Toivanen JT, Timonen J. Estimation of structural and geometrical properties of cortical bone by computerized tomography in 78-year old women. *J Bone Miner Res* 1995;10:139-48.
- Cowin SC. *Bone Biomechanics* (1<sup>st</sup> Ed), Boca Ratón (FL): CRC Press; 1989.
- Skedros JG, Bloebaum RD, Mason MW, Bramble DM. Analysis of a tension/compression skeletal system: possible strain-specific differences in the hierarchical organization of bone. *Anat Rec* 1994;239:393-404.
- Gross TS, Edwards JL, McLeod KJ, Rubin CT. Strain gradients correlate with sites of periosteal bone formation. *J Bone Miner Res* 1997;12:982-8.
- Lai YM, Qin L, Hung VWY, Chan KM. Regional differ-

- ences in cortical bone mineral density in the weight-bearing long bone shaft - A pQCT study. *Bone* 2005;36:465-71.
28. Currey JD. Can strains give adequate information for adaptive bone remodeling? *Calcif Tissue Int* 1984; 36:S118-S122.
  29. Wong M, Carter DR. A theoretical model of endochondral ossification and bone architectural construction in long bone ontogeny. *Anat Embryol* 1990;181:523-32.
  30. Ferretti JL. Peripheral quantitative computed tomography for evaluating structural and mechanical properties of small bone. In: An YH, Draughn RA (eds). *Mechanical Testing of Bone and the Bone-Implant Interface*. Boca Raton (FL): CRC Press; 2000. p385-406.
  31. Ferretti JL, Gaffuri O, Capozza R, Cointy G, Bozzini C, Olivera M, Zanchetta JR, Bozzini CE. Dexamethasone effects on mechanical, geometric and densitometric properties of rat femur diaphysis as described by pQCT and bending tests. *Bone* 1995;16:119-24.
  32. Ferretti JL, Mondelo N, Capozza RF, Cointy GR, Zanchetta JR, Montuori E. Effects of large doses of olpadronate (dimethyl-pamidronate) on mineral density, cross-sectional architecture, and mechanical properties of rat femurs. *Bone* 1995;16(Suppl.):285S-293S.
  33. Capozza RF, Ma YF, Ferretti JL, Meta M, Alippi R, Zanchetta JR, Jee WSS. Tomographic (pQCT) and biomechanical effects of hPTH(1-38) on chronically immobilized or overloaded rat femurs. *Bone* 1995; 17(Suppl.): 233S-239S.
  34. Cointy GR, Mondelo N, Zanchetta JR, Montuori E, Ferretti JL. Intravenous olpadronate restores ovariectomy-affected bone strength. A mechanical, densitometric and tomographic (pQCT) study. *Bone* 1995;17(Suppl.):373S-378S.
  35. Cointy GR, Capozza RF, Negri AL, Ferretti JL. Biomechanical impact of aluminum accumulation on the pre- and post-yield behavior of rat cortical bone. *J Bone Miner Metab* 2005;23:15-23.
  36. Feldman S, Cointy GR, Leite Duarte ME, Sarrió L, Ferretti JL, Capozza RF. Effects of hypophysectomy and recombinant human growth hormone on material and geometric properties and the pre- and post-yield behavior of femurs in young rats. *Bone* 2004;34:203-5.
  37. Ferretti JL, Cointy GR, Capozza RF, Frost HM. Bone mass, bone strength, muscle-bone interactions, osteopenias and osteoporosis. *Mech Ageing Dev* 2003;124:269-79.
  38. Capozza RF, Feldman S, Mortarino P, Reina PS, Schiessl H, Rittweger J, Ferretti JL, Cointy GR. Structural analysis of the human tibia by tomographic (pQCT) serial scans. *J Anat* 2010;216:470-81.
  39. Rittweger J, Goosey-Tokfrey VL, Cointy G, Ferretti JL. Structural analysis of the human tibia in men with spinal cord injury by tomographic (pQCT) serial scans. *Bone* 2010;47:511-8.
  40. Feldman S, Capozza RF, Mortarino P, Reina PS, Ferretti JL, Rittweger J, Cointy GR. Site- and sex-specific effects on tibia structure in long-distance runners and untrained controls. *Med Sci Sports Exerc* 2012;44:1580-8.
  41. Rittweger J, Beller G, Ehrig J, Jung C, Koch U, Ramolla J, Schmidt F, Newitt D, Majumdar S, Schiessl H, Felsenberg D. Bone-muscle strength indices for the human lower leg. *Bone* 2000;27:319-26.
  42. Rittweger J, Michaelis I, Giehl M, Wüseke P, Felsenberg D. Adjusting for the partial volume effect in cortical bone analyses of pQCT images. *J Musculoskel Neuron Interact* 2004;4:436-41.
  43. Smith RW, Walker RR. Femoral expansion in aging women: implications for osteoporosis and fractures. *Science* 1964;145:156-7.
  44. Ashizawa N, Nonaka K, Michikami S, Mizuki T, Amagai H, Tojuyama K, Suzuki M. Tomographical description of tennis-loaded radius: reciprocal relation between bone size and volumetric BMS. *J Appl Physiol* 1999;86:1347-51.
  45. Chigira M. Mechanical optimization of bone. *Med Hypotheses* 1996;46:327-30.
  46. Cordey J, Schneider M, Belendez C, Ziegler WJ, Rahn BA, Perren SM. Effect of bone size, not density, on the stiffness of the proximal part of normal and osteoporotic human femora. *J Bone Miner Res* 1992;7(Suppl.2):S437-S444.
  47. Kontulainen SA, Hughes JM, Macdonald HM, Johnston JD. The biomechanical basis of bone strength development during growth. *Med Sport Sci* 2007;51:13-32.
  48. Haapasalo H, Kontulainen S, Sievänen H, Kannus P, Järvinen M, Vuori I. Exercise-induced bone gain is due to enlargement in bone size without a change in volumetric bone density: a pQCT study of the upper arms of male tennis players. *Bone* 2000;27:351-7.
  49. Heinonen A, Sievänen H, Kyröläinen H, Perttunen J, Kannus P. Mineral mass, size, and estimated mechanical strength of triple jumpers' lower limb. *Bone* 2001; 29:229-85.
  50. Heinonen A, Sievänen H, Kannus P, Oja P, Vuori I. Site-specific skeletal response to long-term weight training seems to be attributable to principal loading modality: a pQCT study of female weightlifters. *Calcif Tissue Int* 2002;70:469-74.
  51. Bass SL, Saxon L, Daly RM, Turner CH, Robling AG, Seeman E, Stuckey S. The effect of mechanical loading on the size and shape of bone in pre-, peri- and post-pubertal girls: a study in tennis players. *J Bone Miner Res* 2002;17:2274-80.
  52. Martin RB, Pickett JC, Zinaich S. Studies of skeletal remodeling in aged men. *Clin Orthop* 1980;149:268-82.
  53. Ruff CB, Hayes WC. Sex differences in age-related remodeling of the femur and tibia. *J Orthop Res* 1988; 6:886-96.
  54. Ward KA, Roy DK, O'Neill TW, Berry JL, Swarbrick CM, Silman AJ, Adams JE. Forearm bone geometry and mineral content in UK women of European and South-Asian origin. *Bone* 2007;41:117-21.
  55. Hasegawa Y, Schneider P, Reiners C, Kushida K, Yamazaki K, Hasegawa K, Nagano A. Estimation of the architectural properties of cortical bone using peripheral quantitative computed tomography. *Osteopor Int* 2000;

- 11:36-42.
56. Ahlborg HG, Johnell O, Turner CH, Rannevik G, Karlsson MK. Bone loss and bone size after menopause. *N Engl J Med* 2003;349:327-34.
  57. Riggs BL, Melton LJ-III, Robb RA, Camp JJ, Atkinson EJ, Peterson JM, Rouleau PA, McCollough CH, Bouxsein ML, Khosla S. Population-based study of age and sex differences in bone volumetric density, size, geometry, and structure at different skeletal sites. *J Bone Miner Res* 2004;19:1945-54.
  58. Nishiyama KK, Macdonald HM, Moore SA, Fung T, Boyd SK, McKay HA. Cortical porosity in boys compared with girls at the distal radius and distal tibia during pubertal growth: an HR-pQCT study. *J Bone Miner Res* 2011;27:273-82.
  59. Russo CR, Lauretani F, Seeman E, Bartali B, Bandinelli S, Di Iorio A, Guralnik J, Ferrucci L. Structural adaptations to bone loss in aging men and women. *Bone* 2006;38:112-8.
  60. Jepsen KJ, Centi A, Duarte GF, Galloway K, Goldman H, Hampson N, Lappe JM, Cullen DM, Greeves J, Izard R, Nindl BC, Kraemer WJ, Negus CH, Evans RK. Biological constraints that limit compensation of a common skeletal trait variant lead to inequivalence of tibial function among healthy young adults. *J Bone Miner Res* 2011;26:2872-65.
  61. Svejme O, Ahlborg HG, Karlsson MK. Changes in forearm bone mass and bone size after menopause. A mean 24-year prospective study. *J Musculoskel Neuronal Interact* 2012;12:192-8.
  62. Negri AL, Barone R, Lombas C, Bogado CE, Zanchetta JR. Evaluation of cortical bone by peripheral quantitative computed tomography in continuous ambulatory peritoneal dialysis patients. *Hemodial Int* 2006;10:351-5.
  63. Weidauer LA, Eilers MM, Binkley TL, Vukovich MD, Specker BL. Effect of different collegiate sports on cortical bone in the tibia. *J Musculoskel Neuronal Interact* 2012;12:68-73.
  64. Martin RB, Atkinson PJ. Age- and sex-related changes in the structure and strength of the human femoral shaft. *J Biomech* 1977;10:223-31.
  65. Burr DB, Martin RB. The effects of composition, structure and age on the torsional properties of the human radius. *J Biomech* 1983;16:603-8.
  66. Boyce TM, Bloebaum RD. Cortical aging differences and fracture implications for the human femoral neck. *Bone* 1993;14:769-78.
  67. Kiebzak GM, Smith R, Gundberg CC, Howe JC, Sacktor B. Bone status of senescent male rats: chemical, morphometric, and mechanical analysis. *J Bone Miner Res* 1988;3:37-45.
  68. Akhter MP, Cullen DM, Recker RR. Bone adaptation response to sham and bending stimuli in mice. *J Clin Densitom* 2002;5:207-16.
  69. Peng ZQ, Väänänen HK, Zhang HX, Tuukkanen J. Long-term effects of ovariectomy on the mechanical properties and chemical composition of rat bone. *Bone* 1997;20:207-12.
  70. Nicholson CL, Firth EC. Assessment of bone response to conditioning exercise in the radius and tibia of young Thoroughbred horses using pQCT. *J Musculoskel Neuron Interact* 2010;10:199-206.
  71. Sugiyama T, Takaki T, Sakanaka K, Sadamaru H, Mori K, Kato Y, Taguchi T, Saito T. Warfarin-induced impairment of cortical bone material quality and compensatory adaptation of cortical bone structure to mechanical stimuli. *J Endocrinol* 2007;194:213-22.
  72. Bonadio J, Jepsen KJ, Mansoura MK, Jaenisch R, Kuhn JL, Goldstein SA. A murine skeletal adaptation that significantly increases cortical bone mechanical properties: Implications for human skeletal fragility. *J Clin Invest* 1993;92:1697-705.
  73. Mikic B, Van der Meulen MCH, Kingsley DM, Carter DR. Mechanical and geometric changes in the growing femur of BMP-5 deficient mice. *Bone* 1996;18:601-7.
  74. Tseng KF, Bonadio JF, Stewart TA, Baker AR, Goldstein SA. Local expression of human growth hormone in bone results in impaired mechanical integrity in the skeletal tissue of transgenic mice. *J Orthop Res* 1996;4:598-604.
  75. Nikander R, Sievänen H, Uusi-Rasi K, Heinonen A, Kannus P. Loading modalities and bone structures at non-weight-bearing upper extremity and weight-bearing lower extremity: A pQCT study of adult female athletes. *Bone* 2006;39:886-94.
  76. Luo G, Cowin SC, Sadegh AM, Arramon YP. Implementation of strain rate as a bone remodeling stimulus. *J Biomech Eng* 1995;117:329-38.
  77. Jepsen KJ, Andarawis-Puri N. The amount of periosteal apposition required to maintain bone strength during aging depends on adult bone morphology and tissue-modulus degradation rate. *J Bone Miner Res* 2012;27:1916-26.
  78. Lorentzon M, Mellström D, Ohlsson C. Association of amount of physical activity with cortical bone size and trabecular volumetric BMD in young adult men: the GOOD Study. *J Bone Miner Res* 2005;20:1936-43.
  79. Felsenberg D, Boonen S. The bone quality framework: determinants of bone strength and their interrelationships, and implications for osteoporosis management. *Clin Ther* 2005;27:1-11.